Heliyon 10 (2024) e39101

Contents lists available at ScienceDirect

Heliyon

journal homepage: www.cell.com/heliyon

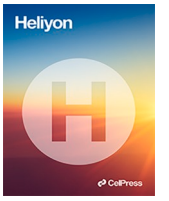

Research article

Tough gelatine hydrogels reinforced with silk fibroin nanofiber

Maho Shibata [a,1], Yoko Okahisa [b,*]

[a] Department of Biobased Materials Science, Graduate School of Science and Technology, Kyoto Institute of Technology, Matsugasaki Sakyo-ku, Kyoto, 606-8585, Japan
[b] Fibre Science and Engineering, Kyoto Institute of Technology, Matsugasaki Sakyo-ku, Kyoto, 606-8585, Japan

ARTICLE INFO

Keywords:
Silk fibroin nanofiber
Gelatine hydrogel
Mechanical properties
Biodegradation

ABSTRACT

Gelatine hydrogels exhibit potential as biomaterials such as wound-healing materials, artificial organs, scaffolds for cell culture and drug delivery systems because of their good biocompatibility. However, their practical applications are limited by their poor mechanical properties and high degradability. In this study, mechanically fibrillated silk fibroin (fibroin nanofibers; FNF) was used to reinforce gelatine hydrogels. The resulting gelatine hydrogels with FNF exhibited enhanced toughness compared to those reinforced with conventional aqueous regenerated fibroin (RF), which were prepared by treatment with a highly concentrated LiBr solvent or a neat gelatine hydrogel while retaining their softness. The average pore size of the gelatine hydrogel was 2.2 μm, while the gelatine hydrogel containing 25 % FNF expanded to 6.7 μm. A web-like network was formed between the pores. The addition of FNF increased the relative β-sheet contents in the hydrogels to 60.3 %, suggesting that this may have caused structural changes such as increased crystallinity for gelatine-derived proteins. Furthermore, the addition of FNF inhibited the rapid enzymatic degradation of gelatine hydrogels. FNF, which can be easily prepared in water, is a safe material for both the environment and living organisms and holds promise as a biomaterial in the future.

1. Introduction

Gelatine hydrogels hold potential as biomaterials for applications such as wound-healing materials, artificial organs, scaffolds for cell culture and drug delivery systems, owing to their high biocompatibility. However, their practical applications are limited by their low mechanical strength and high degradability [1]. Consequently, extensive research has been conducted to improve the properties of gelatine hydrogels via crosslinking or compositing with other polymers [1–4]. In particular, polysaccharide-reinforced hydrogels have been widely reported, demonstrating that strong hydrogels can be obtained by compositing with bacterial cellulose (BC) and nanocellulose [5–7]. Despite their effectiveness as cell culture substrates and wound dressings in vitro, these polysaccharide-reinforced gels may pose compatibility issues for in vivo use as the human body lacks cellulolytic enzymes [8]. Therefore, a reinforcing material with higher biological safety is needed for in vivo applications.

Fibroin, a fibrous protein, is the main component of silkworm cocoons. Owing to its toughness and biocompatibility, fibroin has previously been complexed with gelatine [9–12]. For complexation with gelatine, fibroin fibres must be dissolved in a solvent. Because fibroin is not soluble in water, highly concentrated salt solvents such as lithium bromide are generally utilised. This necessitates a

* Corresponding author.
E-mail address: okahisa@kit.ac.jp (Y. Okahisa).
[1] Present address: ZEBRA CO., LTD.

https://doi.org/10.1016/j.heliyon.2024.e39101
Received 27 May 2024; Received in revised form 5 September 2024; Accepted 7 October 2024
Available online 10 October 2024

desalting dialysis process to eliminate toxicity, which is time-consuming and requires substantial amounts of water.

Recently, we have successfully produced mechanically fibrillated fibroin, i.e., fibroin nanofiber (FNF) aqueous dispersions, via mechanical treatment using only water [13]. This technique allows fibroin fibres to be dispersed in water without undergoing dissolution and regeneration processes [14]. FNFs maintain their native crystal and β-sheet structures and exhibit excellent mechanical properties and heat resistance [14–17]. Given these properties, water-dispersed FNF may be effective in reinforcing water-containing hydrogels. In this study, we aimed to reinforce gelatine hydrogels with FNFs.

2. Materials and methods

An aqueous dispersion of FNFs was prepared from degummed fibroin (provided by Nagasuna Mayu Inc., Kyoto, Japan) by grinding with water as described previously [13]. Briefly, degummed fibroin and water were passed four times through a grinder (MKCA6–3, Masko Sangyo Co., Japan) at 1500 rpm with grinding stones (NKGC6–120, Masko). The resultant FNFs, dispersed in water, were referred to as the FNF aqueous dispersion. The diameters of the obtained FNFs ranged from 60 to 150 nm, as previously reported [13, 14]. As a control, aqueous RF solutions were obtained using a 9 M lithium bromide solution and subsequently subjected to desalting dialysis [18]. Degummed fibroin was dissolved in the 9 M lithium bromide solution and dialyzed in running water for 3 d to desalinate. The resulting RF solution was clear and light yellow. Gelatine powder was added to the FNF aqueous dispersion or RF solution and stirred at 1000 rpm for 1 h at 55 °C. After stirring, the solution was thoroughly mixed using an ultrasonicator at 750 W and 20 kHz for 1 min. The utilised fibroin/gelatine (w/w) ratios were 0/100 (G100), 5/95 (F5G95), 10/90 (F10G90), 15/85 (F15G85), 20/80 (F20G80), and 25/75 (F25G75). Since uncross-linked gelatine hydrogel is sensitive to temperature changes and softens even at room temperature, physical property tests cannot be accurately used for comparing reinforcement effects. Therefore, glutaraldehyde cross-linking was used in this study. Glutaraldehyde, a 5-carbon aliphatic molecule with aldehyde groups at both ends, is widely used as a cross-linker for collagen or gelatine because of its high reactivity and high solubility in aqueous solutions, despite concerns about its toxicity and that of other chemical cross-linkers [19]. It was chosen for this study because it facilitates the comparison of the reinforcing effects of FNF and RF. Glutaraldehyde was added as a cross-linking agent to the fibroin/gelatine mixture at a concentration of 0.8 mmol per 1 g of protein and then stirred at 150 rpm for 40 s. The produced hydrogel was left to stand overnight in a refrigerator at 3 °C.

Morphological observations were performed using a Hitachi S-3400N scanning electron microscopy (SEM) at 10 kV. The gels were frozen in liquid nitrogen and lyophilized to minimize changes in pore size due to ice crystal growth. The image obtained from SEM observation was binarized using ImageJ, an image processing open-source software, to obtain the area of the pore area, and then the diameter was calculated assuming that the pores were circular. Fifteen pore diameters were obtained for each sample, and the average was calculated. Fourier-transform (FTIR) spectroscopy was used to analyse the secondary structures in the attenuated total reflection mode by conducting 32 scans with a resolution of 4 cm^{-1} (Spectrum One, Parkin Elmer Japan G.K.). Fourier self-deconvolution was performed by fitting the amide I peak with a Gaussian function, and the β-sheet fraction was calculated as described elsewhere [20,21]. The mechanical properties of the fabricated hydrogels were determined via compression testing with the elastic modulus calculated using a creep metre at a compression rate of 0.05 mm/s, a relative humidity of 90 %, and 15 repetitions (RE-3305s; Yamaden Co., Ltd.). The rupture strength and strain were calculated using a universal testing machine at a compression rate of 60 mm/min, a maximum compression distance of 9 mm, and eight repetitions (EZ-SX: Shimadzu).

The swelling ratio of each hydrogel was calculated by measuring the ratio of the weight after immersion in phosphate-buffered saline (PBS) to the weight after drying. Hydrogels measuring 1 cm^2 were prepared, completely immersed in pH 7.4 PBS, and placed in a refrigerator at 6 °C for 24 h. After removal from the PBS, the PBS on the surface was wiped off, and the hydrogel was weighed to determine the swollen weight (W_s). The swollen hydrogels were then lyophilized and weighed again to determine the dry weight (W_d). Ten hydrogels were prepared for each condition and measured. The degree of swelling was calculated from the values of W_s and W_d according to the following formula:

$$\text{Swelling ratio} = \frac{W_s - W_d}{W_d} \tag{1}$$

In vitro biodegradation studies of G100, FNF-F15G85, and RF-F15G85 were performed according to a previously established protocol with slight modifications [21]. Pre-weighted hydrogel samples cut into 5 mm cubes were incubated with 157.2 mg of protease (*Streptomyces griseus*-Type XIV, P5147, 5.3 u/mg: Sigma-Aldrich, Merck KGaA, Darmstadt, Germany) and 0.88 μg of collagenase (Collagenase Type 2, CLS2, 260 u/mg: Worthington Biochemical Corporation, NJ, USA) with or without 1 mL of PBS at 37 °C. The samples were removed from the enzyme solution at specific time intervals, washed with distilled water, lyophilized, and weighed. The degree of biodegradation was determined via the following equation:

$$\text{Degradation ratio (\%)} = \left(1 - \frac{W_t \times R_{wd}}{W_i}\right) \times 100 \tag{2}$$

where W_t is the dry weight of the hydrogel after the enzymatic treatment. W_i is the wet weight of the hydrogel before the enzymatic treatment. R_{wd} is the wet/dry hydrogel ratio calculated as follows:

$$\text{wet} \Big/ \text{dry ratio} = \frac{\text{Wet weight of hydrogel without enzymatic treatment}}{\text{Dry weight of hydrogel without enzymatic treatment}} \tag{3}$$

3. Results and discussions

The SEM images of the cut cross-sections and the average pore size of the obtained gels are shown in Figs. 1 and 2. In the FNF-gelatine samples, a web-like network was formed between the pores. This network structure expanded with an increasing FNF amount up to 15 wt% (Fig. 1a and b), whereas FNF-F20G80 and FNF-F25G75 were similar to FNF-F15G75 (Fig. 1c–e). A previous study reported that web-like network structures were formed via glutaraldehyde cross-linking in silk gels prepared using an RF solution [20]. In this study, fine network structures were observed in RF-F10G90 and RF-F20/G80 (Fig. 1i and j), but not in RF-F25G75 (Fig. 1k). Meanwhile, a clear network structure was formed in FNF-F25G75 (Fig. 1e and f). Notably, FNFs are not soluble in water but exist in a dispersed state, which indicates that FNFs maintained their nanofiber shape in the prepared gels. The average pore size of G100 was 2.2 μm. The pore size increased with an increasing fibroin addition rate, regardless of FNF or RF. It has been reported that as the gelatine concentration in the composite increases, more lamellar structural layers form, resulting in smaller pore sizes [22,23]. In this study, the addition of FNF and RF reduced the amount of gelatine in the composite hydrogel, likely resulting in a larger pore diameter. Moreover, the pore sizes of the FNF–gelatine samples, e.g., 6.7 μm for FNF-F25G75, were larger than those of the RF-gelatine gels; for example, RF-F25G75 had a pore size of 5.2 μm (Fig. 2). The FNF maintained its nanofiber shape and formed a network structure in the gel, which may have contributed to the difference in pore sizes. These results reveal that the pore size varied with the addition of fibroin, indicating that the scaffold pore size can be modulated by fibroin addition. The range of pore sizes suitable for different types of cellular activities varies significantly [24]. Therefore, gelatine hydrogels for specific cell differentiation can be prepared from fibroin–gelatine gels.

The results of FTIR analyses of the prepared gels are shown in Fig. 3. For the protein material, characteristic vibrational bands are observed at 1650 cm^{-1} for amide I due to C=O stretching, at 1550 cm^{-1} for amide II due to C–N–H stretching, and at 1400–1200 cm^{-1} for amide III due to N–H bending [25]. The positions of these peaks obtained for the gelatine gels prepared in this study differ considerably (Fig. 3a). The relative percentages of β-sheets were calculated from the areas of the β-sheet bands (at approximately 1630 cm^{-1}) in the amide I region (Fig. 3b and c). For the FNF–gelatine gels, the peak areas derived from the β-sheet structures are

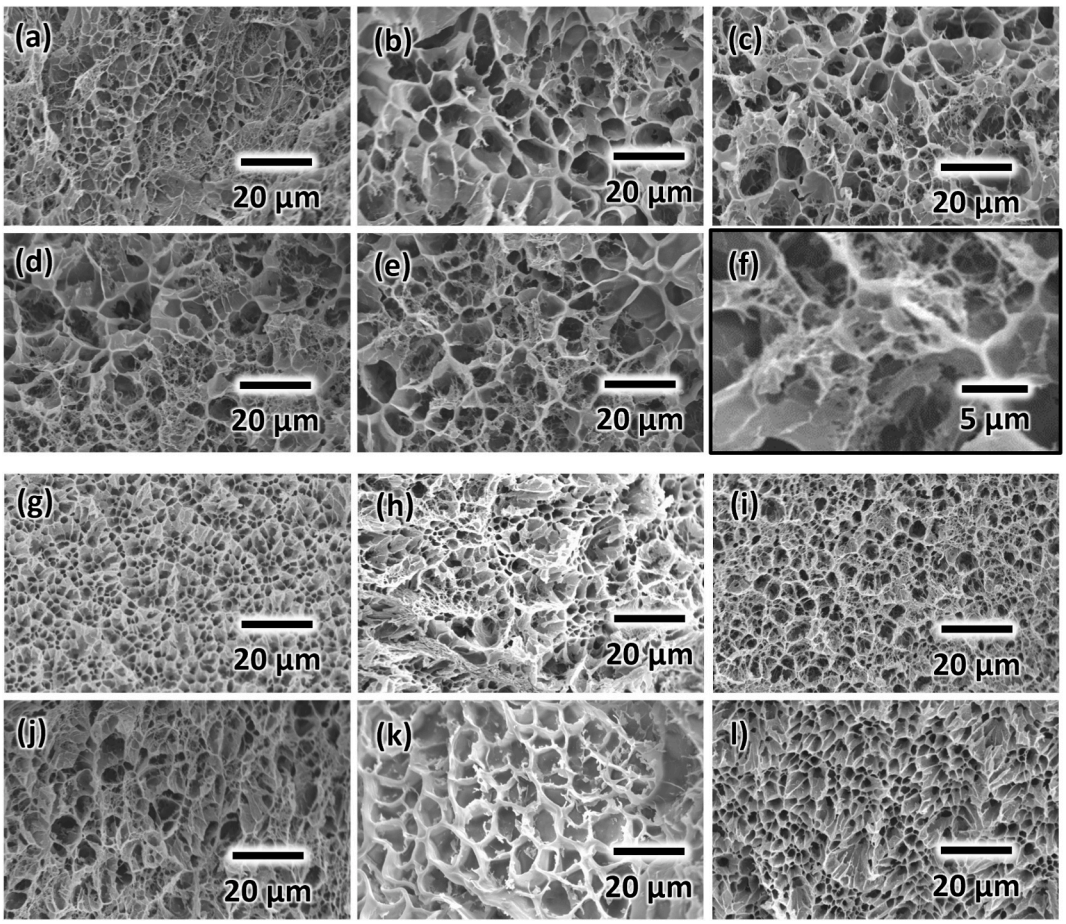

Fig. 1. SEM images of the dry hydrogel cross-sections: (a) FNF-F5G95, (b) FNF-F10G90, (c) FNF-F15G85, (d) FNF-F20G80, (e) FNF-F25G75, (f) FNF-F25G75 (enlarged), (g) RF-F5G95, (h) RF-F10G90, (i) RF-F15G85, (j) RF-F20G80, (k) RF-F25G75, and (l) G100.

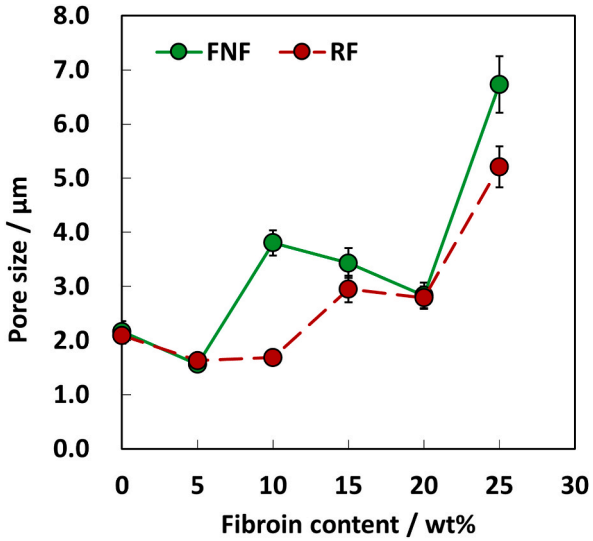

Fig. 2. Average pore size of the dry hydrogel cross-sections. Error bars show standard deviations.

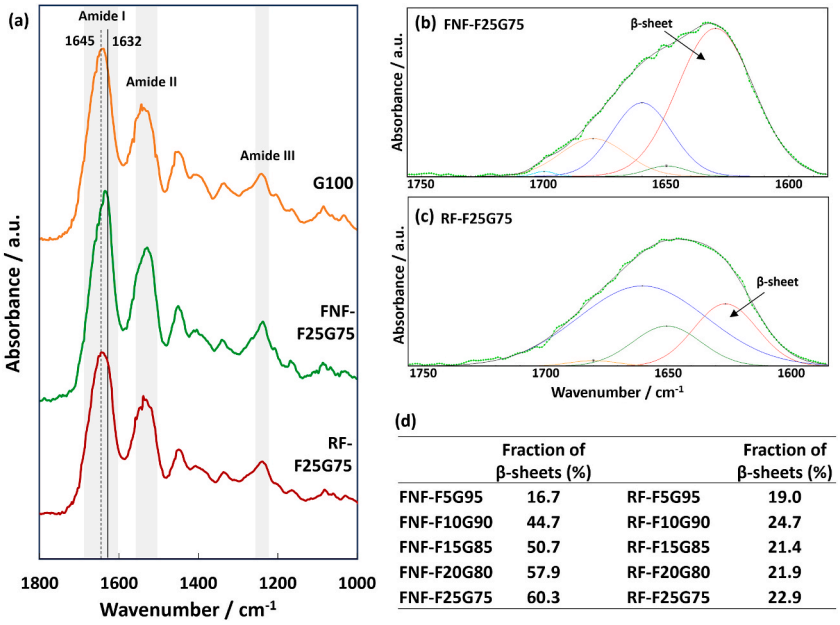

(d)

	Fraction of β-sheets (%)		Fraction of β-sheets (%)
FNF-F5G95	16.7	RF-F5G95	19.0
FNF-F10G90	44.7	RF-F10G90	24.7
FNF-F15G85	50.7	RF-F15G85	21.4
FNF-F20G80	57.9	RF-F20G80	21.9
FNF-F25G75	60.3	RF-F25G75	22.9

Fig. 3. (a) Typical FTIR spectra of the dried G100, FNF−gelatine, and RF-gelatin hydrogels. Fourier self-deconvolution of the amide I region for calculating the relative β-sheet contents in (b) FNF–gelatine and (c) RF−gelatine. (d) Relative contents of β-sheets in the dried hydrogels.

significantly larger than those of the RF−gelatine gels, and the fraction of β-sheets increased with increasing FNF content. This suggests that the addition of FNF changed the structural properties of the gelatine-derived proteins, such as their crystallinity. Gelatine normally forms a triple-helix structure upon gelation; however, it has been reported that a β-sheet structure can also form under certain conditions. Sakai et al. found that the elasticity of gelatine gels increased approximately 10-fold when gelatine gelation occurred in a micro-sized lipid space. Furthermore, they found that smaller microgels contained more β-sheet structures than the normal bulk gel, which made the gels stiffer [26]. In this study, complexation with FNF may have induced the formation of β-sheet structures in gelatine gels. Meanwhile, for the RF−gelatine samples, the fractions of β-sheets did not change significantly after increasing the RF amount, suggesting that RF did not promote gel crystallization.

The results of the compression tests conducted on the prepared gels are shown in Fig. 4. The fracture strength and strain of the FNF−gelatine gels are higher than those of neat G100 (Fig. 4a) and increase with an increase in the FNF addition rate from 5 to 15 wt% (Fig. 4b). In the FNF–gelatine hydrogels, the interactions between nanofibers or between nanofibers and gelatine likely formed a network structure, inhibiting the growth of microcracks in gelatine hydrogels and thus increasing their compressive strength. In

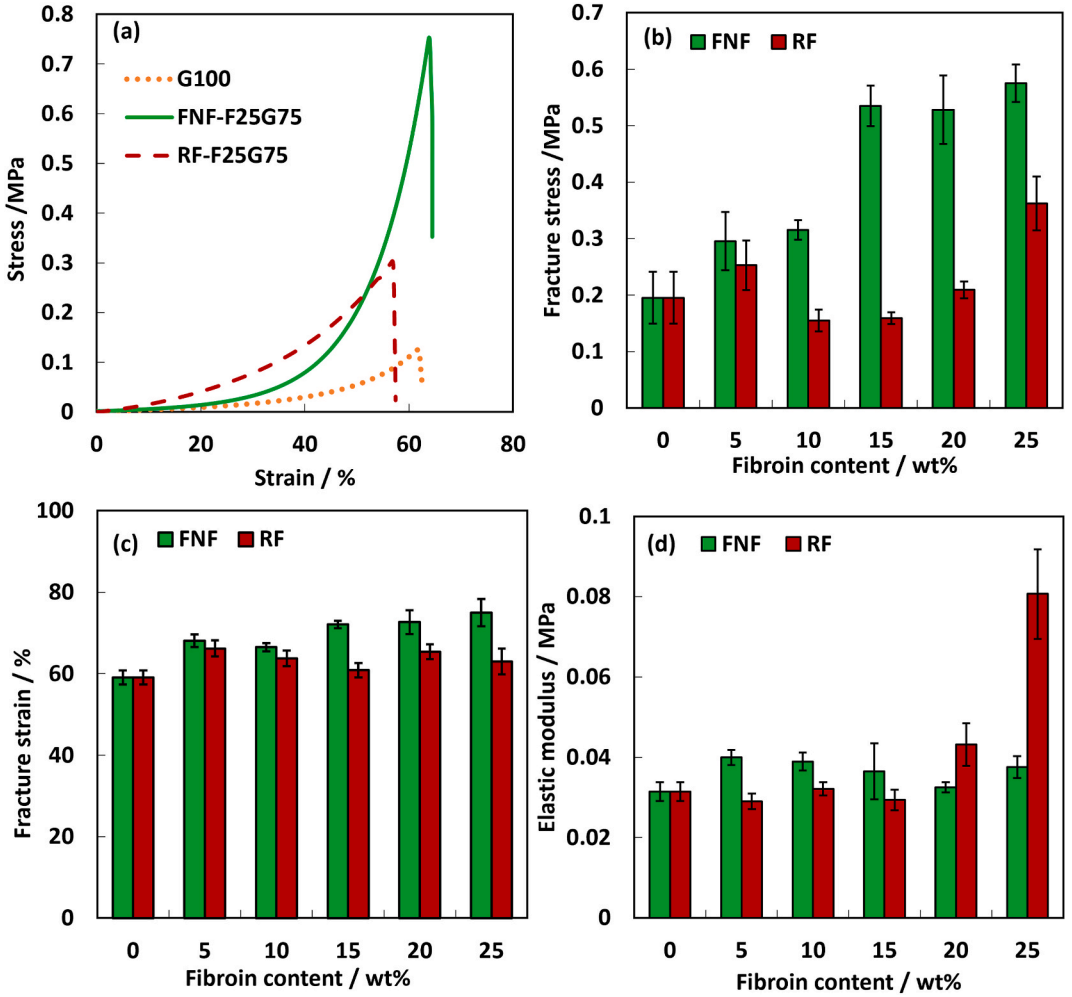

Fig. 4. (a) Typical stress–strain curves recorded during the compression tests conducted for the G100, FNF–gelatine, and RF–gelatine hydrogels. (b) Fracture strengths, (c) fracture strains, and (d) elastic moduli of various hydrogels. Error bars show standard deviations.

contrast, the stress and strain of the gels with 15, 20, and 25 wt% FNF remained stable. SEM observations also revealed that these gels had similar structures, suggesting that FNFs did not contribute to the gel strength improvement at contents greater than 15 wt% owing to inhomogeneous aggregation [4]. For the RF–gelatine samples, increasing the added fibroin amount did not improve the compressive strength and strain as significantly as for the FNF–gelatine samples. According to the obtained SEM images, the RF network structure was smaller than that of FNFs, which may explain the absence of a reinforcement effect. Meanwhile, the elastic modulus of the FNF–gelatine hydrogels remained almost unchanged, whereas that of the RF–gelatine hydrogels increased with the addition of more than 20 % fibroin (Fig. 4c). Therefore, FNF increased the hydrogel's toughness while maintaining its softness.

The results of the swelling ratio of each gel are shown in Fig. 5. In this study, both FNF and RF had little effect on the swelling ratio, although previous reports indicate that complexing SF with hydrophobic β-sheet domains reduces the degree of gelatine swelling [27–29]. One possible reason for this discrepancy might be that the glutaraldehyde cross-linking had already reduced the degree of swelling of the gelatine. Glutaraldehyde crosslinking is known to induce a significant reduction in swelling [30]. Hydrogels prepared by other crosslinking methods, such as genipin, enzymes, and photocrosslinkable crosslinking, may exhibit similar effects on the degree of swelling as previously reported.

The gel degradation rates are shown in Fig. 6. The sample without fibroin was almost completely degraded in 24 h, whereas the sample containing 15 wt% fibroin retained more than 50 % of its original content even after 24 h. Although gelatine hydrogels exhibit good biodegradability, they degrade too quickly for some applications, such as scaffolds and drug delivery systems; therefore, their degradation time must be properly controlled. The biodegradation rates of gelatine hydrogels could be adjusted using fibroin (Fig. 6). The remaining fibroin, which is less susceptible to enzymatic degradation than gelatine, may have inhibited degradation by preventing enzymes from entering the hydrogel.

The rapid increase in the hydrogel degradation rate between 0 and 2 h may be due to the presence of soluble components that did not form a network structure in the gel and leaked into the soaking solution. Similarly, Li et al. observed a rapid weight loss

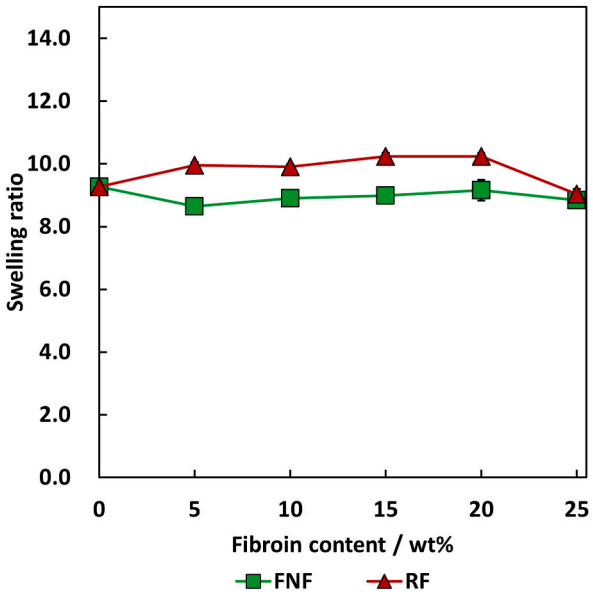

Fig. 5. Swelling ratios of the G100, FNF-gelatine, and RF-gelatine hydrogels. Error bars show standard deviations.

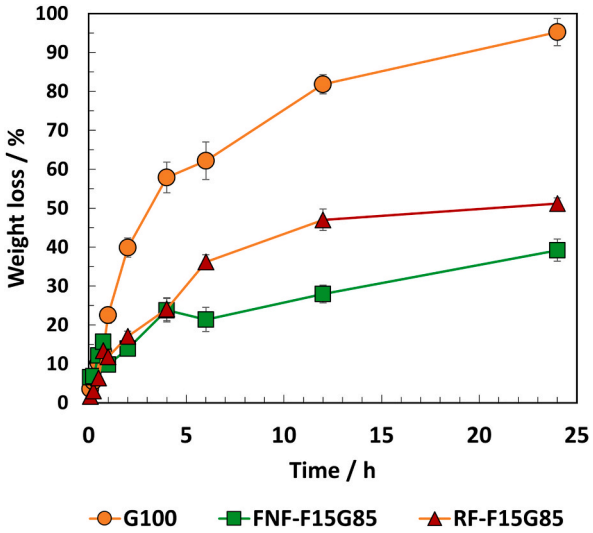

Fig. 6. Biodegradation rates of the G100, FNF-F15G85, and RF-F15G85 hydrogels obtained within 24 h. Error bars shows standard deviations.

immediately after the immersion of fibroin sheets in protease XIV, followed by a slower degradation process [31]. Horan et al. reported that protease XIV eroded fibroin from the hydrogel surface and that the diameter of fibroin fibres decreased with the immersion time [32]. FNF, which still retains its fibre shape and high crystallinity, may have degraded more slowly than RF.

In summary, the addition of FNFs resulted in gelatine hydrogels that were less prone to fracture while maintaining their softness, compared to gelatine hydrogels with or without RF. Furthermore, FNFs inhibited the rapid degradation of gelatine hydrogels and adjusted their pore size. FNFs, which can be easily prepared using only water, are environmentally safe and biocompatible, making them an excellent reinforcing component for biomaterials. These tough hydrogels have the potential to be used as wound-healing materials by adding high functionality to gelatine or FNF by loading metal nanoparticles [33]. Moreover, hydrogels possess a three-dimensional structure that mimics the extracellular matrix (ECM) of the body, making them suitable as scaffold materials and drug delivery carriers containing cell growth factors. Cell proliferation is known to be affected by the elasticity of solid tissues [34]. In this study, FNF reinforcement increased the toughness of the hydrogels without altering the elastic modulus, which may not interfere with cell culture in conventional gelatine hydrogels. Moreover, the polymeric nanofiber matrix, with its nanoscaled nonwoven fibrous ECM proteins, is a candidate ECM-mimetic material [35]. In the case of FNF, cell adhesion may be improved because of their nanofiber shape, and further studies are needed to verify these functions.

4. Conclusion

In this study, we aimed to reinforce gelatine hydrogels with a FNF aqueous dispersion, which we recently developed, and compared them with conventional hydrogels complexed with dissolved regenerated fibroin. In all samples, a pore structure of a few micrometres in diameter was observed. The pore size tended to increase with increasing fibroin addition rate, particularly in the sample with FNF, where the pore size was relatively larger than that of RF gel, and a web-like network was observed between the pores. FTIR analysis suggested that the addition of FNF may have caused some changes in the structure of gelatine-derived proteins, such as an increase in crystallinity. In contrast, the ratio of the β-sheet structure did not change significantly with increasing amounts of RF in the RF-complexed gel, suggesting that RF has no effect on promoting gel crystallization. The compression test results showed that the gelatine hydrogel was less prone to fracture without softness loss compared to the gelatine hydrogels with and without fibroin when RF was added. Enzymatic biodegradability tests indicated that the addition of fibroin inhibits the rapid degradation of gelatine hydrogels in vivo. FNFs, which are easily prepared using only water, are safe for both the environment and living organisms and hold promise as an excellent reinforcing material for biomaterials. On the other hand, there are concerns about the toxicity of glutaraldehyde, which was used as a cross-linking agent in this study, and it is difficult to put the hydrogels produced in this paper to practical use as is. It is necessary to use cross-linking agents other than glutaraldehyde, such as genipin or enzymes, which are biologically safe. Moreover, the difference in the reinforcing effect of FNF on these materials also needs to be verified.

CRediT authorship contribution statement

Maho Shibata: Validation. **Yoko Okahisa:** Writing – review & editing, Validation, Conceptualization.

Declaration of competing interest

The authors declare that they have no known competing financial interests or personal relationships that could have appeared to influence the work reported in this paper.

Acknowledgment

We are grateful to Mr. Kazuki Horii and Mr. Osamu Nagasuna from Nagasuna Mayu Inc. for their generous donation of the fibroin samples. We would like to thank Dr. Isao Wataoka from the Kyoto Institute of Technology for useful discussions.

Appendix A. Supplementary data

Supplementary data to this article can be found online at https://doi.org/10.1016/j.heliyon.2024.e39101.

References

[1] P. Taheri, R. Jahanmardi, M. Koosha, S. Abdi, Physical, mechanical and wound healing properties of chitosan/gelatin blend films containing tannic acid and/or bacterial nanocellulose, Int. J. Biol. Macromol. 154 (2020) 421–432, https://doi.org/10.1016/j.ijbiomac.2020.03.114.
[2] R. Dash, M. Foston, A.J. Ragauskas, Improving the mechanical and thermal properties of gelatin hydrogels cross-linked by cellulose nanowhiskers, Carbohydr. Polym. 91 (2013) 638–645, https://doi.org/10.1016/j.carbpol.2012.08.080.
[3] K. Yue, G. Trujillo-de Santiago, M.M. Alvarez, A. Tamayol, N. Annabi, A. Khademhosseini, Synthesis, properties, and biomedical applications of gelatin methacryloyl (GelMA) hydrogels, Biomaterials 73 (2015) 254–271, https://doi.org/10.1016/j.biomaterials.2015.08.045.
[4] W. Wang, X. Zhang, A. Teng, A. Liu, Mechanical reinforcement of gelatin hydrogel with nanofiber cellulose as a function of percolation concentration, Int. J. Biol. Macromol. 103 (2017) 226–233, https://doi.org/10.1016/j.ijbiomac.2017.05.027.
[5] S. Cui, S. Zhang, S. Coseri, An injectable and self-healing cellulose nanofiber-reinforced alginate hydrogel for bone repair, Carbohydr. Polym. 300 (2023) 120243, https://doi.org/10.1016/j.carbpol.2022.120243.
[6] N. Naseri, B. Deepa, A.P. Mathew, K. Oksman, L. Girandon, Nanocellulose-Based interpenetrating polymer network (IPN) hydrogels for cartilage applications, Biomacromolecules 17 (2016) 3714–3723, https://doi.org/10.1021/acs.biomac.6b01243.
[7] A. Nakayama, A. Kakugo, J.P. Gong, Y. Osada, M. Takai, T. Erata, S. Kawano, High mechanical strength double-network hydrogel with bacterial cellulose, Adv. Funct. Mater. 14 (2004) 1124–1128, https://doi.org/10.1002/adfm.200305197.
[8] N. Lin, A. Dufresne, Nanocellulose in biomedicine: current status and future prospect, Eur. Polym. J. 59 (2014) 302–325, https://doi.org/10.1016/j.eurpolymj.2014.07.025.
[9] E.S. Gil, R.J. Spontak, S.M. Hudson, Effect of β-sheet crystals on the thermal and rheological behavior of protein-based hydrogels derived from gelatin and silk fibroin, Macromol. Biosci. 5 (2005) 702–709, https://doi.org/10.1002/mabi.200500076.
[10] M.C.T. Asuncion, J.C.-H. Goh, S.-L. Toh, Anisotropic silk fibroin/gelatin scaffolds from unidirectional freezing, Mater. Sci. Eng. C. 67 (2016) 646–656, https://doi.org/10.1016/j.msec.2016.05.087.
[11] W. Xiao, J. Li, X. Qu, L. Wang, Y. Tan, K. Li, H. Li, X. Yue, B. Li, X. Liao, Cell-laden interpenetrating network hydrogels formed from methacrylated gelatin and silk fibroin via a combination of sonication and photocrosslinking approaches, Mater. Sci. Eng. C. 99 (2019) 57–67, https://doi.org/10.1016/j.msec.2019.01.079.
[12] G. Kulkarni, P. Guha Ray, P.K. Byram, M. Kaushal, S. Dhara, S. Das, Tailorable hydrogel of gelatin with silk fibroin and its activation/crosslinking for enhanced proliferation of fibroblast cells, Int. J. Biol. Macromol. 164 (2020) 4073–4083, https://doi.org/10.1016/j.ijbiomac.2020.09.016.
[13] Y. Okahisa, C. Narita, K. Yamada, Preparation of silk-fibroin nanofiber film with native β-sheet structure via a never dried-simple grinding treatment, J. Fiber Sci. Technol. 75 (2019) 29–34, https://doi.org/10.2115/fiberst.2019-0005.

[14] Y. Okahisa, Y. Yasunaga, K. Iwai, S. Yagi, K. Abe, I. Nishizawa, S. Ifuku, Optically transparent silk fibroin nanofiber paper maintaining native β-sheet secondary structure obtained by cyclic mechanical nanofibrillation process, Mater. Today Commun. 29 (2021) 102895, https://doi.org/10.1016/j.mtcomm.2021.102895.
[15] Y. Yasunaga, Y. Aso, K. Yamada, Y. Okahisa, Preparation of transparent fibroin nanofibril-reinforced chitosan films with high toughness and thermal resistance, Carbohydr. Polym. Technol. Appl. 5 (2023) 100299, https://doi.org/10.1016/j.carpta.2023.100299.
[16] Y. Okahisa, C. Narita, T. Aoki, Surface analysis of novel fibroin films based on well-preserved crystalline structures, Int. J. Biol. Macromol. 191 (2021) 1017–1025, https://doi.org/10.1016/j.ijbiomac.2021.09.125.
[17] Y. Okahisa, C. Narita, K. Yamada, Fabrication and characterization of a novel silk fibroin film with UV and thermal resistance, Mater. Today Commun. 25 (2020) 101630, https://doi.org/10.1016/j.mtcomm.2020.101630.
[18] D.N. Rockwood, R.C. Preda, T. Yücel, X. Wang, M.L. Lovett, D.L. Kaplan, Materials fabrication from Bombyx mori silk fibroin, Nat. Protoc. 6 (2011) 1612–1631, https://doi.org/10.1038/nprot.2011.379.
[19] K. Adamiak, A. Sionkowska, Current methods of collagen cross-linking: review, Int. J. Biol. Macromol. 161 (2020) 550–560, https://doi.org/10.1016/j.ijbiomac.2020.06.075.
[20] Y. Lin, X. Xia, K. Shang, R. Elia, W. Huang, P. Cebe, G. Leisk, F. Omenetto, D.L. Kaplan, Tuning chemical and physical cross-links in silk electrogels for morphological analysis and mechanical reinforcement, Biomacromolecules 14 (2013) 2629–2635, https://doi.org/10.1021/bm4004892.
[21] R. Batra, R. Purwar, Deduction of a facile method to construct Antheraea mylitta silk fibroin/gelatin blend films for prospective biomedical applications, Polym. Int. 70 (2021) 73–82, https://doi.org/10.1002/pi.6087.
[22] M. Nieto-Suárez, M.A. López-Quintela, M. Lazzari, Preparation and characterization of crosslinked chitosan/gelatin scaffolds by ice segregation induced self-assembly, Carbohydr. Polym. 141 (2016) 175–183, https://doi.org/10.1016/j.carbpol.2015.12.064.
[23] A. Mirtaghavi, A. Baldwin, N. Tanideh, M. Zarei, R. Muthuraj, Y. Cao, G. Zhao, J. Geng, H. Jin, J. Luo, Crosslinked porous three-dimensional cellulose nanofibers-gelatine biocomposite scaffolds for tissue regeneration, Int. J. Biol. Macromol. 164 (2020) 1949–1959, https://doi.org/10.1016/j.ijbiomac.2020.08.066.
[24] Q.L. Loh, C. Choong, Three-dimensional scaffolds for tissue engineering applications: role of porosity and pore size, Tissue Eng. Part B Rev. 19 (2013) 485–502, https://doi.org/10.1089/ten.teb.2012.0437.
[25] A. Barth, Infrared spectroscopy of proteins, Biochim. Biophys. Acta - Bioenerg. 1767 (2007) 1073–1101, https://doi.org/10.1016/j.bbabio.2007.06.004.
[26] A. Sakai, Y. Murayama, K. Fujiwara, T. Fujisawa, S. Sasaki, S. Kidoaki, M. Yanagisawa, Increasing elasticity through changes in the secondary structure of gelatin by gelation in a microsized lipid space, ACS Cent. Sci. 4 (2018) 477–483, https://doi.org/10.1021/acscentsci.7b00625.
[27] E.S. Gil, D.J. Frankowski, R.J. Spontak, S.M. Hudson, Swelling behavior and morphological evolution of mixed gelatin/silk fibroin hydrogels, Biomacromolecules 6 (2005) 3079–3087, https://doi.org/10.1021/bm050396c.
[28] W. Xiao, J. He, J.W. Nichol, L. Wang, C.B. Hutson, B. Wang, Y. Du, H. Fan, A. Khademhosseini, Synthesis and characterization of photocrosslinkable gelatin and silk fibroin interpenetrating polymer network hydrogels, Acta Biomater. 7 (2011) 2384–2393, https://doi.org/10.1016/j.actbio.2011.01.016.
[29] L. Wang, L. Yan, S. Liu, H. Zhang, J. Xiao, Z. Wang, W. Xiao, B. Li, X. Liao, Conformational transition-driven self-folding hydrogel based on silk fibroin and gelatin for tissue engineering applications, Macromol. Biosci. 22 (2022) 2200189, https://doi.org/10.1002/mabi.202200189.
[30] A. Bigi, G. Cojazzi, S. Panzavolta, K. Rubini, N. Roveri, Mechanical and thermal properties of gelatin films at different degrees of glutaraldehyde crosslinking, Biomaterials 22 (2001) 763–768, https://doi.org/10.1016/S0142-9612(00)00236-2.
[31] M. Li, M. Ogiso, N. Minoura, Enzymatic degradation behavior of porous silk fibroin sheets, Biomaterials 24 (2003) 357–365, https://doi.org/10.1016/S0142-9612(02)00326-5.
[32] R.L. Horan, K. Antle, A.L. Collette, Y. Wang, J. Huang, J.E. Moreau, V. Volloch, D.L. Kaplan, G.H. Altman, In vitro degradation of silk fibroin, Biomaterials 26 (2005) 3385–3393, https://doi.org/10.1016/j.biomaterials.2004.09.020.
[33] H. Liang, M.S. Mirinejad, A. Asefnejad, H. Baharifar, X. Li, S. Saber-Samandari, D. Toghraie, A. Khandan, Fabrication of tragacanthin gum-carboxymethyl chitosan bio-nanocomposite wound dressing with silver-titanium nanoparticles using freeze-drying method, Mater. Chem. Phys. 279 (2022) 125770, https://doi.org/10.1016/j.matchemphys.2022.125770.
[34] A.L. Zajac, D.E. Discher, Cell differentiation through tissue elasticity-coupled, myosin-driven remodeling, Curr. Opin. Cell Biol. 20 (2008) 609–615, https://doi.org/10.1016/j.ceb.2008.09.006.
[35] Z. Ma, M. Kotaki, R. Inai, S. Ramakrishna, Potential of nanofiber matrix as tissue-engineering scaffolds, Tissue Eng. 11 (2005) 101–109, https://doi.org/10.1089/ten.2005.11.101.